

Research Article

Formation of Germanium Nitride Nanowires on the Surface of Crystalline Germanium

David Jishiashvili, Lasha Kiria, Zeinab Shiolashvili, Nino Makhatadze, Elguja Miminoshvili, and Alexander Jishiashvili

Institute of Cybernetics, Georgian Technical University, 5 Euli Street, 0186 Tbilisi, Georgia

Correspondence should be addressed to David Jishiashvili; d.jishiashvili@gtu.ge

Received 29 March 2013; Revised 30 May 2013; Accepted 1 June 2013

Academic Editor: Mingwang Shao

Copyright © 2013 David Jishiashvili et al. This is an open access article distributed under the Creative Commons Attribution License, which permits unrestricted use, distribution, and reproduction in any medium, provided the original work is properly cited.

We report on the growth mechanisms of germanium nitride nanowires on the surface of crystalline Ge annealed in hydrazine vapor at different temperatures. In spite of the presence of water (and hence oxygen precursors) in hydrazine, the pure germanium nitride single crystal nanowires were produced in the temperature range of 480–580°C. At temperatures below 520°C, the GeO_x clusters were formed first at the Ge surface, followed by the nucleation and growth of nanowires through the Vapor-Liquid-Solid mechanism. The Vapor-Solid growth mechanism was observed at temperatures exceeding 520°C, and Ge₃N₄ nanobelts were produced instead of nanowires with circular cross-sections. All nanostructures have the alpha germanium nitride structure; however, at the nucleation stage, the presence of beta Ge₃N₄ phase was also observed in the roots of nanowires.

1. Introduction

Nanowire-based devices are considered nowadays as one of the most promising alternatives to conventional micro-electronic facilities, which can promote further shrinking of device sizes and increase their functionality. The unique properties of one-dimensional (1D) nanowires arise due to their low dimensionality and hence by quantum-mechanical properties and surface dominated features. From the technological point of view, they have one more advantage. Due to high aspect ratios, the length of nanowires lies in the micrometer range reaching even millimeter sizes. Such “large” elements can be easily handled and manipulated when building different nanodevices and circuits.

Germanium nitride has attracted much attention in recent years due to its unique properties and potential applications in different devices [1–3]. It can be used as a thin film material for the passivation of different semiconductors in metal-insulator-semiconductor devices [2, 4–8], as a buffer layer to grow the crystalline GaN film on Ge [9], material for plasmonic devices [1], effective nonoxide photocatalyst for overall water splitting [10], and stable negative electrode material for Li-ion batteries [11]. A new

cubic spinel-structured phase of Ge₃N₄ (γ -phase) is harder than sapphire and can be used as a hard material [12]. As for the growth of one-dimensional germanium nitride nanostructures, there are only two papers dealing with Ge₃N₄ nanobelts and nanowires (NWs) [13, 14] produced at 850°C. Earlier, we presented the preliminary results on the growth of nanostructured germanium nitride at significantly lower temperatures [15]. The purpose of this work is to investigate the initial stages of formation, growth mechanisms, structure, and morphology of Ge₃N₄ nanowires produced at temperatures below 580°C.

2. Materials and Methods

Germanium nitride nanowires were grown on the surface of a single-crystal Ge source, which was cut from Ge ingot using the diamond saw without any other surface treatment or polishing. The application of unpolished Ge surfaces with several micrometer size irregularities increased the surface area and hence the yield of nanowires. Besides, the large surface roughness eliminated the influence of surface orientation on the growth rate of nanowires. As a result, at similar process parameters the morphology, structure, and average

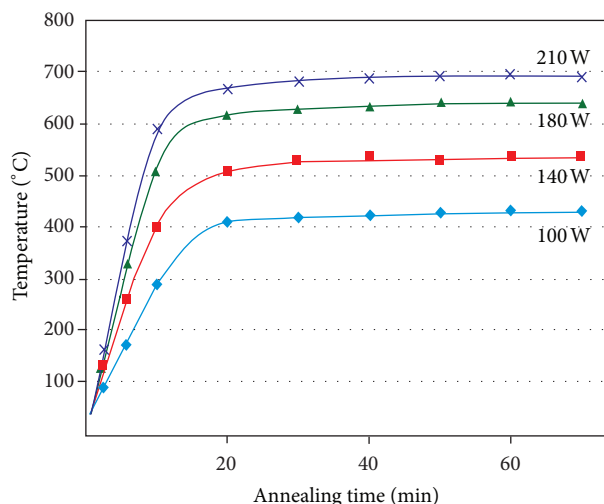


FIGURE 1: Dependence of Ge source temperature on the applied power.

yield of nanowires were the same for Ge sources with different surface orientation. For example, the yield of nanowires was $\sim 5.7 \text{ mg/cm}^2 \cdot \text{h}$ at 530°C in spite of the surface orientation of Ge sources. Most of experiments were performed using the (111) oriented 2 mm thick Ge sources placed on the bottom of the vertical quartz reactor and heated up to 580°C using the external resistive furnace. The quartz tube was first evacuated down to 4×10^{-5} Torr and then filled with N_2H_4 vapor, which contained 3 mol.% H_2O . The saturated pressure of N_2H_4 (~ 10 Torr) was established in the chamber at room temperature, because the water content in hydrazine was too small to alter the pressure value of N_2H_4 . The reactor was then isolated from the vacuum system, and the external furnace was switched on. At temperatures close to 480°C , the reactivity of water impurities prevailed causing the formation of oxides at the Ge surface. At elevated temperatures, the Ge surface served as catalyst, and N_2H_4 was decomposed through the fast chain reactions, forming active transient nitrogen precursors (NH_2 , NH , N) until finally the stable NH_3 , N_2 and H_2 molecules were formed [16]. The chemical synthesis of Ge_3N_4 in the water diluted hydrazine vapor has a complex nature, as it involves several reagents with different phases (solid Ge, gaseous H_2O , N_2H_4 , and its decomposition products). The detailed analysis of complex reactions which leads to the synthesis of Ge_3N_4 nanowires forms a separate scientific task which is under study at present. Some details of the previously described new technology are presented elsewhere [15, 17].

The morphology and structure of NWs were studied using FEI Quanta FEG 600 Scanning Electron Microscope (SEM) and Philips CM200 FEG Transmission Electron Microscope (TEM). XRD data were taken on a Shimadzu XRD-6000 diffractometer.

3. Results and Discussion

During annealing in hydrazine vapor, the temperature of Ge source depended on the power which was applied to

the external furnace. After the furnace was switched on, the source temperature was rising gradually and then stabilized reaching the saturation value T_S (Figure 1). The temperature ramps also depended on the applied power and varied from $21^\circ\text{C}/\text{min}$ at 120 W ($T_S = 480^\circ\text{C}$) to $36^\circ\text{C}/\text{min}$ at 160 W ($T_S = 580^\circ\text{C}$). Typically, the growth processes lasted for 45–60 min in the temperature range of 480 – 580°C . These annealing temperatures were insufficient to melt or sublime neither Ge with the melting temperature of $T_m = 936^\circ\text{C}$ nor its dioxide GeO_2 ($T_m = 1230^\circ\text{C}$ [18]) or nitride Ge_3N_4 [19, 20]. Considering the interaction of Ge with ambient vapor, one may conclude that the only volatile species which can be produced in this temperature range are GeO monoxide molecules. GeO molecules can be easily formed due to interaction of Ge with water, and they readily sublime even at 400°C [21]. As the maximum annealing temperature in our experiments does not exceed 580°C , we supposed that the whole Ge mass transfer in our growth processes was accomplished through these volatile GeO molecules.

To study the growth processes in details, the Ge sources were annealed at different temperatures in the range of 480 – 580°C , and the products, which were growing on the Ge surface at each temperature, were analyzed.

SEM image of Ge source surface annealed for 4 hours at 480°C in hydrazine vapor with 3 mol.% water is shown in Figure 2(a). The white balls with diameters ranging from 0.1 up to micrometers are observed, and they are scattered all over the Ge surface. According to XRD and Auger analysis (the results are not presented) only Ge and oxygen atoms are found at the surface, and the diamond like Ge source is the only existing crystalline phase. The spherical shapes of particles indicate that before solidification they were molten drops which do not wet the Ge source. As it was mentioned earlier, 480°C is insufficient temperature to melt Ge or GeO_2 . However, it is well known that depending on composition, the off-stoichiometric oxides (suboxides) and nitrides may have sufficiently low melting temperature [22, 23]. These results lead to the conclusion that the oxygen is concentrated mainly in balls consisting of amorphous Ge suboxides which are formed during annealing in the presence of water molecules.

To explain the preferential formation of oxide at 480°C , the possible chemical reactions for producing Ge oxides and nitrides from the existing precursors (H_2O , hydrazine decomposition products) were thermodynamically evaluated and compared (the thermodynamic data were obtained from software HSC chemistry 5.0). The preliminary evaluations reveal that all these reactions have negative change in Gibbs free energy (ΔG) and are therefore thermodynamically favorable at 480°C . The maximum negative value of ΔG (-1609 kJ/mol) was obtained when NH molecules were used for the synthesis of Ge_3N_4 . However, besides the sign of ΔG , the yield of the final reaction product in this multicomponent system strongly depends on the rates of oxidation or nitridation reactions. For silicon, which is the structural analogue of Ge, the wet oxidation is the well-established technology for the fast production of thick SiO_2 layers. In the presence of H_2O molecules the oxidation of Si is much more rapid than dry oxidation and it proceeds with a high linear rate

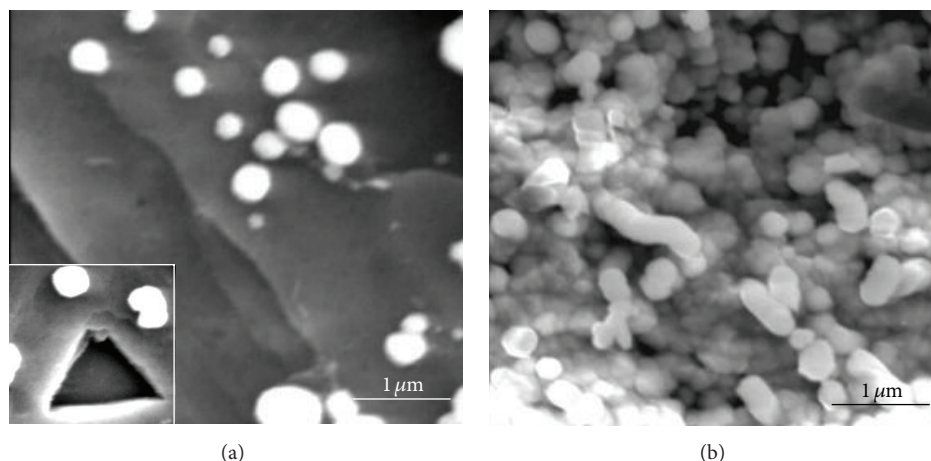


FIGURE 2: Formation of GeO_x balls and clusters on the surface of Ge source annealed at 480°C in hydrazine containing 3 mol.% H_2O (a) and 5 mol.% H_2O (b). Inset shows one of the triangular etch pits formed on the (111) Ge surface after annealing in hydrazine.

constant (6.2×10^8 versus $6.2 \times 10^6 \mu\text{m}/\text{h}$) and with a less activation energy (0.78 versus 1.23 eV) [24]. The wet oxidation was applied also to Ge [25, 26] and significant increase in the growth rate was observed which obeyed a nearly cubic law [25]. It was found that at a room temperature the dissociative adsorption of water molecules takes place both on GeO_2 and Ge surfaces [27, 28]. The subsequent transfer of OH to the Ge- GeO_2 interface promotes the process of oxidation. The effective reversible reaction of Ge with water ($\text{Ge} + \text{H}_2\text{O} = \text{GeO} + \text{H}_2$) was used for the formation of an intensive flux of volatile GeO molecules and growth of epitaxial Ge film with the maximum rate of $9 \mu\text{m}/\text{h}$ [29, 30]. These results confirm the high oxidation rate of Ge in the presence of water. In contrast to H_2O , the adsorption of NH_3 molecules on Ge surface was not observed [31]. Taking into consideration the previously mentioned aspects, we assume that in our technology the kinetic factors that are high oxidation rate of Ge in the presence of H_2O prevail over the large negative Gibbs free energy values of nitride forming reactions. As a result, the layer of GeO_x balls is formed on the Ge surface at 480°C , as it is indicated in Figure 2.

The small amount of water in hydrazine (3 mol.%) is sufficient only to form suboxide molecules instead of stable dioxides with high melting points. The increase of water content up to 5 mol.% is still insufficient for producing GeO_2 , but it intensifies the process, causing formation of a layer of suboxide balls on the surface of Ge source (Figure 2(b)).

It is well known that when reacting with Ge, the water molecules serve as active oxidizers as well as a reducers providing volatile GeO molecules for the mass transfer and growth of different nanostructures like Ge- GeO_2 core-shell nanowires and even for the formation of polycrystalline Ge films [29, 32, 33]. Annealing of Ge- GeO_2 system in conditions similar to our experiments provides a high pressure of GeO vapor ($\sim 10^{-5}$ Torr) and intensive VLS growth of Ge NWs from the catalyst GeO_x ball tips [34]. The deep triangular etch pit is clearly seen in the inset of Figure 2(a). The etch pits of these shapes are characteristic features of Ge (111)

surface etching. The results presented in Figure 2 prove that in our experiments the water molecules are actively eroding Ge, forming the intensive flux of volatile monoxide molecules which then serve as precursors for the growth of nitride nanowires.

Figure 3 presents the SEM images of Ge sources annealed in hydrazine at 500°C . At this temperature, the nanowires begin to grow directly on the surfaces of agglomerated GeO_x balls as it is shown in Figures 3(a) and 3(b). Near the basis, the NWs are twisted making many turns but they are quite straight at some distance above the basis. The NWs were growing like bushes (Figure 3(c)), and after 2 hours of growth, a thick mat of nanowires was formed on the Ge source surface (Figure 3(d)).

At this stage, following precursors were presented at the surface of Ge source: GeO_x ball-shaped clusters (possibly with local Ge droplets or local small areas with high Ge content); nitrogen precursors (N, NH, NH_2 , NH_3); gaseous GeO, water, and hydrogen molecules.

It is worth noting that hydrogen actively reduces the GeO_x surface [35] and produces the pure Ge which may be mixed with GeO_x . Besides, the pure Ge may be produced also due to the phase separation in monoxide which follows the reaction: $2\text{GeO} = \text{Ge} + \text{GeO}_2$. In the presence of hydrogen and hence in the presence of the hydrazine decomposition products, this last reaction proceeds even at 350°C [35] promoting the formation of Ge atoms which may then react with chemically active gaseous precursor or enrich the GeO_x cluster.

Further investigations reveal that depending on the source temperature the growth of NWs may proceed by two mechanisms. At low temperatures not exceeding 510°C , the molten Ge-rich GeO_x nanodroplets serve as self-catalysts and promote the growth of NWs through the classic Vapor-Liquid-Solid (VLS) mechanism. The molten droplets are actively adsorbing nitrogen precursors and GeO molecules. A part of GeO is easily reduced to Ge in the presence of

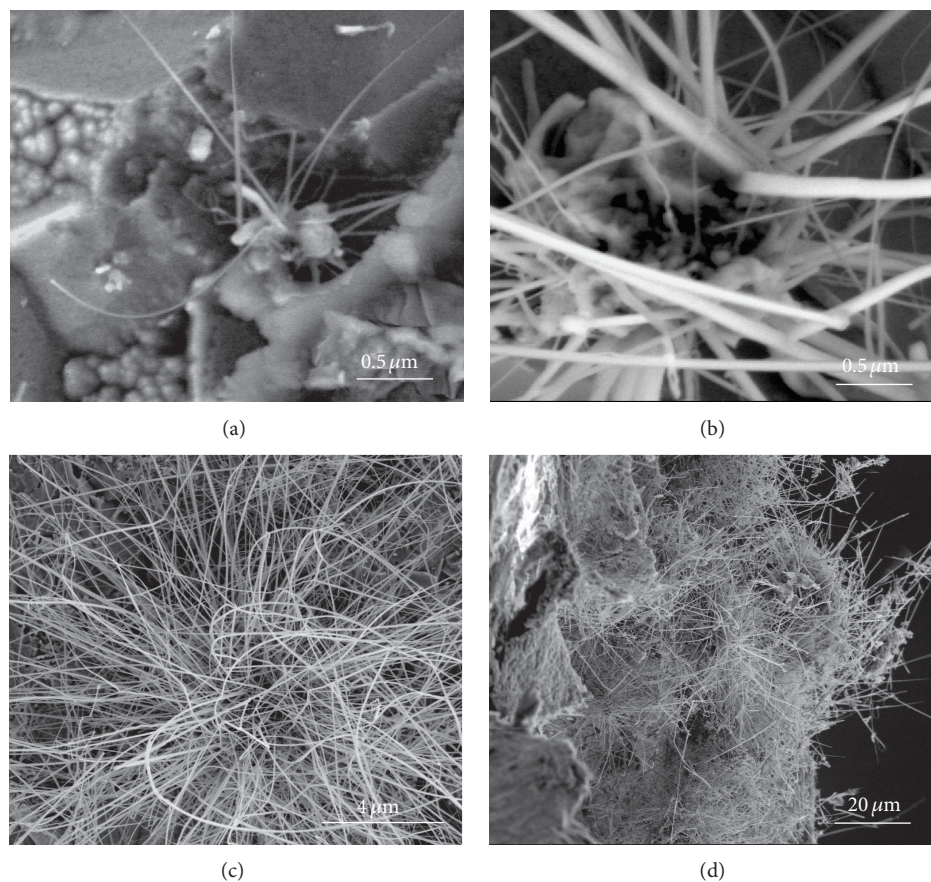


FIGURE 3: Ge_3N_4 nanowires growing from GeO_x balls at the initial stage of annealing at 500°C ((a), (b)); nanowires growing in the form of a bush (c); the mat of nanowires formed on the Ge source after 2 h of growth.

hydrogen, supplying the droplet with Ge. The absorbed nitrogen precursors oversaturate the catalyst, and after diffusion through it they precipitate at the growth front forming solid Ge_3N_4 . The VLS mechanism needs low energy budget and dominates at temperatures close to 500°C .

The TEM images and the electron diffraction pattern of nanowires grown at 500°C are presented in Figure 4. The catalyst droplets can be clearly seen at the top of germanium nitride nanowires. The formation of $\alpha\text{-Ge}_3\text{N}_4$ nanowires (space group: $P31c$) was confirmed by XRD method (the results of XRD are presented below in Figure 7(a)) and by electron diffraction patterns; one example of which is presented in Figure 4(d). The interplanar distances calculated from these electron diffraction patterns were compared with data obtained in [36] for the most intense XRD lines (data presented in [36] are shown in square brackets): (102)-0.275 nm [0.277 nm]; (201)-0.296 nm [0.305 nm]; (211)-0.240 nm [0.245 nm].

The plain growth front is clearly defined at the catalyst-nanowire interface (Figure 4(c)). It covers nearly the whole cross-section of nanowire. The droplet itself consists of a dark core surrounded with a bright shell. This core-shell structured tip is formed after solidification of the molten catalyst. Earlier [15], it was established that for small droplets with diameters not exceeding ~ 12 nm, the solidification may

cause the segregation of Ge and GeO_x phases and the appearance of significant compressive pressure. As a result of this pressure, the Ge nanoparticle with a dense, unusual tetragonal structure was formed at the tip of a nanowire which was surrounded with an amorphous GeO_x sheath. The size of droplet in Figure 4(c) exceeds 12 nm, and we consider that the core comprises amorphous Ge, while the shell is an amorphous GeO_x . The contrast in this TEM image is caused by differences in average atomic numbers between Ge and GeO_x (Z-contrast).

The composition of nanowire tips were investigated using the energy dispersive X-ray analysis (EDX). To eliminate the signal from the Ge source the nanowires were scratched of the source, and placed on the Si substrate. The nanowires with large tips were selected for the analysis, and the results of elemental mapping are presented in Figures 5(a)–5(d). A small part of nanowire body was also included in the analyzed area (Figures 5(a)–5(d)) to clearly show the differences in composition between the tip and body. The nitrogen related signal from the tip is quite weak but strong in the region of nanowire body (Figure 5(d)). The overall Ge signal is relatively uniform with a slightly brighter tip region (Figure 5(c)). The oxygen is distributed more or less evenly all over the Si substrate and nanowire, while the tip has a slightly intense color (Figure 5(b)). Figure 5(e) represents the EDX spectrum

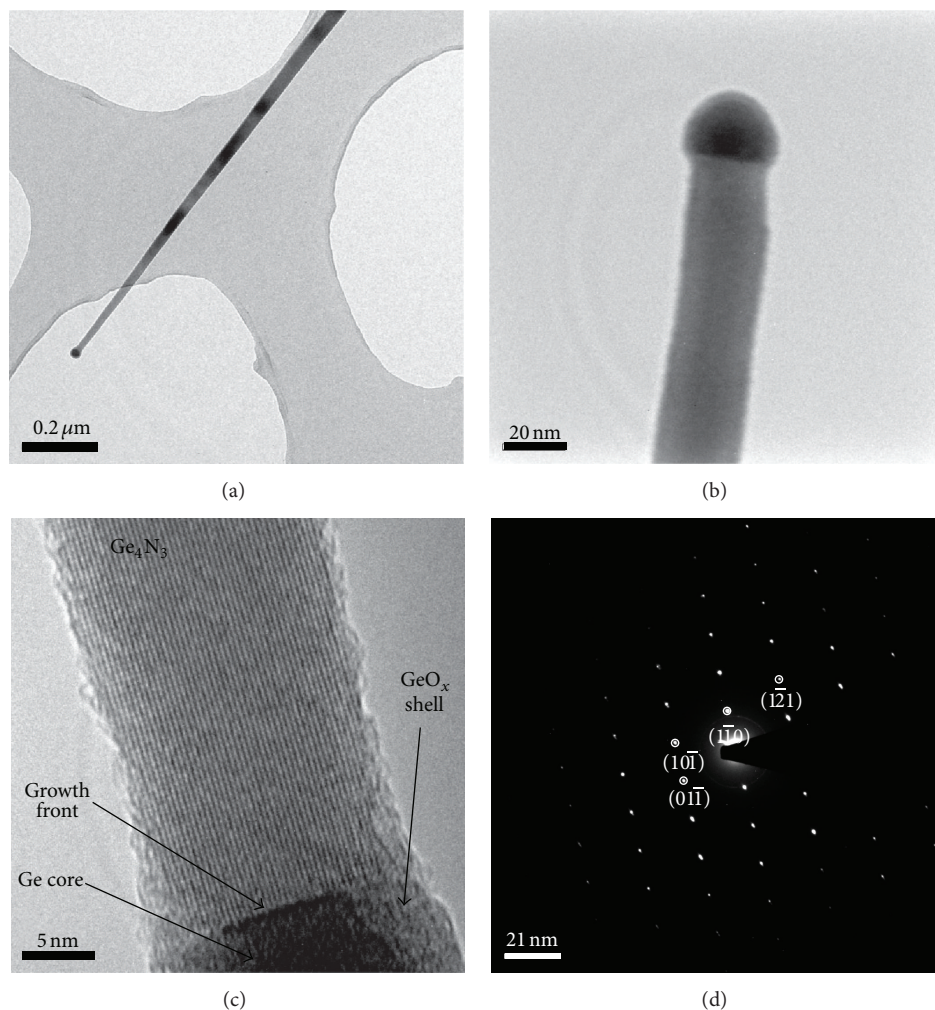


FIGURE 4: TEM images of nanowires grown at 500°C ((a), (b)); HRTEM image of the nanowire and catalyst tip (c); electron diffraction pattern of Ge_3N_4 nanowire, zone axis (111) (d).

of the nanowire tip, and its close area, which is marked by the dashed rectangular in Figure 5(a). The peak of silicon originates from the Si substrate underneath the nanowire. The spectrum proves once again that the Ge is the main constituent of a tip and it contains a small amount of oxygen and less amount of nitrogen, possibly in the form of the adsorbed layer.

A slight tapering of nanowires is observed in Figures 4(a)–4(c). The side wall deposition of Ge_3N_4 and direct synthesis of nitride at the walls should be eliminated as a reason for tapering, because the temperature is too low for the synthesis of germanium nitride from gaseous precursors. On the other hand, the thickness of growing nanowire mat shown in Figure 3(d) increases with time, screening the catalyst tip from GeO molecules evaporated from the Ge source underneath. The feeding of catalyst with Ge precursors gradually decreases, while the amount of gaseous nitrogen precursors impinging the tip is almost constant within the growth time. As a result, a part of Ge in the molten catalyst tip is consumed for the growth of NWs causing the decrease

of a tip size and hence the tapering of nanowires. This means that the reduction of the flux of GeO molecules to the catalyst droplet is the main limiting factor of the growth. The minimum diameter of VLS grown Ge_3N_4 nanowire was 7 nm, and the maximum observed length was several micrometers.

At temperatures exceeding 510°C, the Ge nitride may be formed at the surface by direct reaction between gaseous GeO molecules and nitrogen precursors leading to the growth through the Vapor-Solid (VS) mechanism. However, in this case, depending on the Ge source temperature, the grown nanostructures are nanobelts or faceted nanowires as it is shown in Figure 6. The large discrepancy in widths of nanostructures were observed even for nanobelts grown at the same source temperature (Figures 6(a) and 6(b)).

The high resolution TEM images and electron diffraction patterns of VS grown nanobelts prove their good crystallinity (Figures 6(c), 6(d), and 6(e)). HRTEM image of the nanobelt with the minimum thickness of approximately two atomic layers is shown in Figure 6(c). This nanobelt was grown at 520°C. It should be noted that at intermediate temperatures

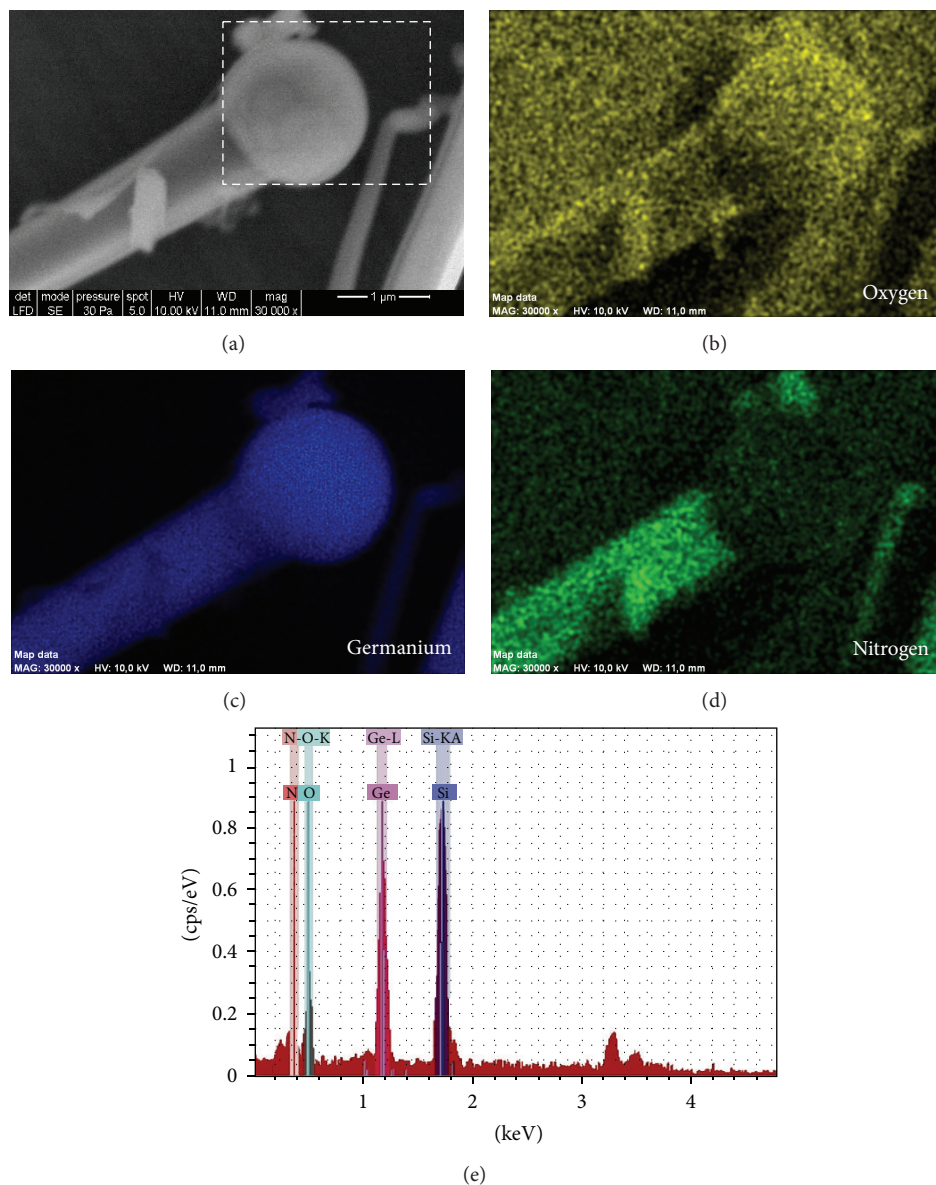


FIGURE 5: SEM image of VLS grown Ge_3N_4 nanowire (a) and corresponding elemental mapping ((b)–(d)); (e) EDX spectrum of a tip, obtained from the dashed rectangular indicated in (a).

in the range of 510–520 °C both VLS and VS nanowires coexist at the source, possibly due to some local thermal fluctuations at the Ge surface.

At growth temperatures exceeding 540 °C, the most of NWs were faceted having different cross-sections and shapes beginning from triangular to hexagonal (Figures 6(f), 6(h), and 6(i)). The cross-section of grown nanostructures strongly depended on the growth temperature as it is shown in Figures 6(f)–6(i). Large, micrometer-sized crystalline blocks of Ge_3N_4 were formed after annealing at 580 °C. Most of these blocks have bodies of elongated irregular hexagonal prisms with distorted hexagonal pyramids at the tips (Figures 6(f) and 6(i)). The observed crystal habits can be attributed to the well-known acicular and blade like hexagonal habits which

are characterizing the “equilibrium” growth of hexagonal crystals with minimum total surface free energy [37].

Figure 6(d) and inset in it represent the high resolution TEM image of nanobelt and its fast Fourier transform. The spots in the inset were indexed and calculated d-spacings confirmed the formation of $\alpha\text{-Ge}_3\text{N}_4$. Besides, it is clearly seen that the nanobelt is growing in the direction perpendicular to the (01-1) plane. More than 30 Ge_3N_4 nanowires were analyzed by TEM method. It should be noted that all these nanowires were growing in the direction perpendicular to (01-1) plane, and all of them have the structure of $\alpha\text{-Ge}_3\text{N}_4$ in spite of their growth mechanism or morphology. The structures of micrometer-sized Ge nitrides obtained at high temperatures and scratched off the Ge sources were analyzed

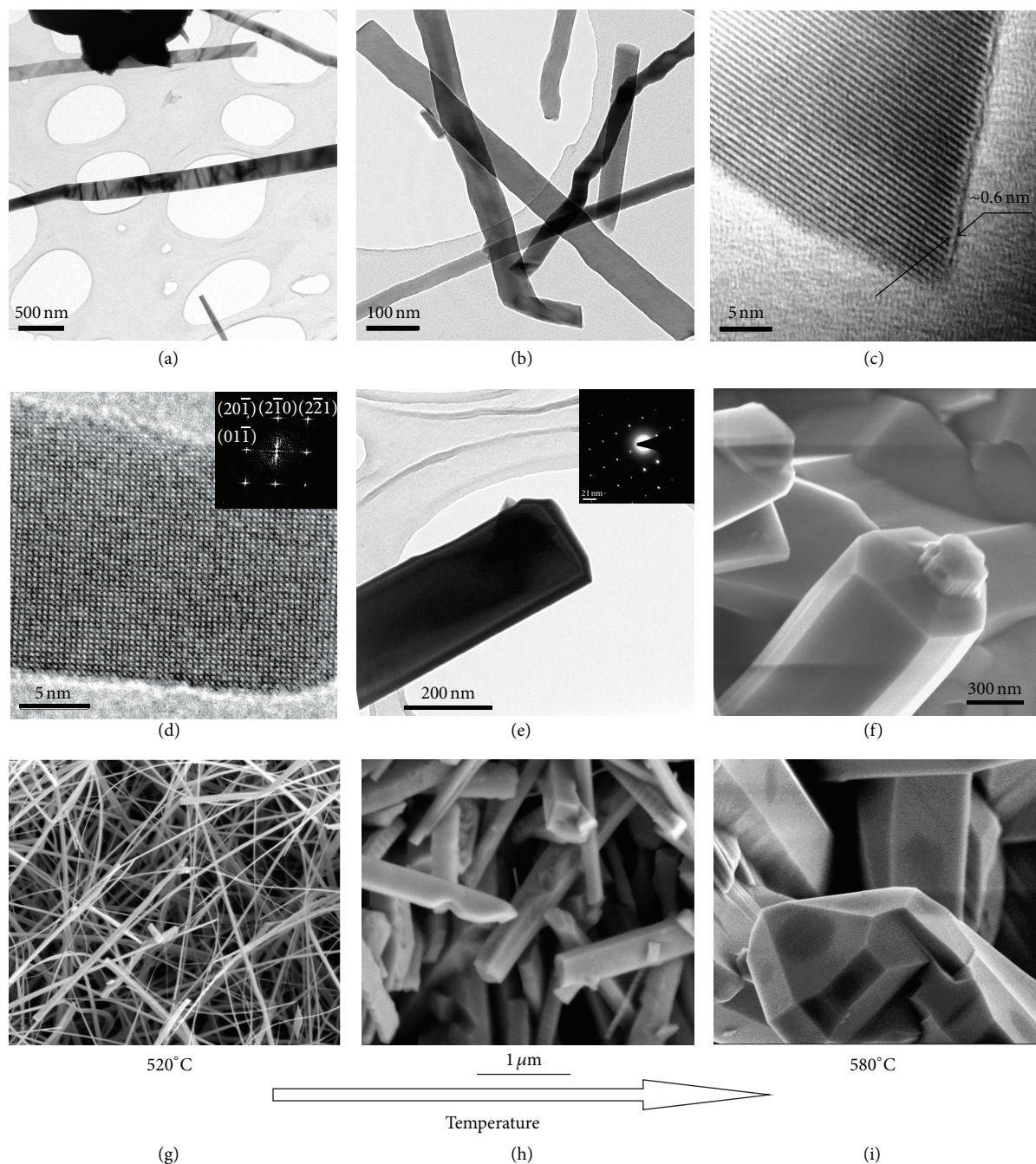


FIGURE 6: TEM ((a), (b), and (e)) and HRTEM ((c), (d)) images of Ge_3N_4 nanobelts synthesized at 520°C . Insets in (d) and (e) represent fast Fourier transform and electron diffraction pattern of respective images; SEM picture of a crystalline Ge_3N_4 formed at 580°C (f); SEM images of nanowires grown at different temperatures ((g), (h), and (i)).

by XRD method which also confirmed the formation of $\alpha\text{-Ge}_3\text{N}_4$ phase.

Theoretically, Ge_3N_4 can exist in at least five possible structures, that is, α , β , γ , pseudocubic, and graphitic phases [38]. α and β phases are more energetically favorable than other phases (γ phase is produced only at very high pressures). The total energy difference between β - and γ - Ge_3N_4 is quite large— 0.27 eV per structural unit, but when comparing β - and α - Ge_3N_4 , the difference is negligibly small,

only 0.006 eV/unit [2, 39]. Due to this small difference the β phase is considered to be more stable than α ; however, when the structure is transformed from α - to β - Ge_3N_4 , the gain in energy is quite small. One possible explanation for the exceptional growth of α - Ge_3N_4 nanowires in our experiments implies that in accordance with the empirical Ostwald's rule of stages, the first crystalline phase during precipitation may be the less stable polymorph [37]. This may be due to kinetic factors (higher nucleation and growth

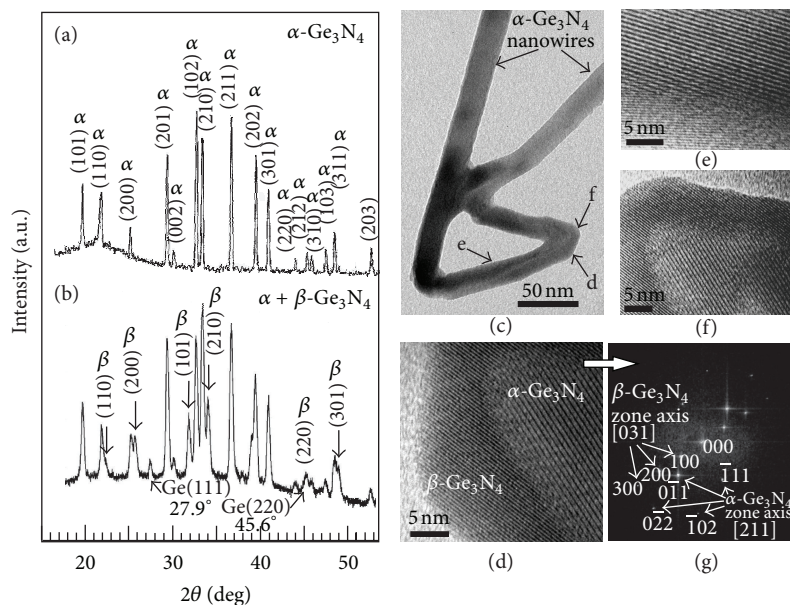


FIGURE 7: XRD patterns of nanowires scratched off the substrate (a) and attached to the Ge source (b); TEM image of Ge_3N_4 nanowire root (c); HRTEM images of points marked on (c) with letters “d,” “e,” and “f” ((d)–(f)); (g) represents the fast Fourier transform of (d). The arrows in (g) are indicating the spots of α - and β - Ge_3N_4 phases.

rates of α phase) because kinetics are often more important than thermodynamics in the nonequilibrium precipitating systems. It should be mentioned that from the available two publications describing the growth of 1D Ge_3N_4 nanomaterials at 850°C , only α -phase nanowires were synthesized in [14], and α - and β - Ge_3N_4 nanobelts were produced in [13]. These results confirm that the stability of α - Ge_3N_4 nanowires is quite high. The temperatures in our processes were at least by 300°C lower in comparison with those used in [13, 14]. We suppose that in our technology after the first solid α - Ge_3N_4 appears from the molten catalyst in VLS process or at the surface of Ge or GeO_x in VS process, its further growth proceeds as an epitaxial growth from the liquid or vapor phase, and the formed α - Ge_3N_4 nanostructures remain stable during the whole growth and cooling processes. In spite of this, the traces of β - Ge_3N_4 were also found in our experiments, and the details of their formation will be considered below.

As it was mentioned previously, no nanowires with phases other than α - Ge_3N_4 were found by TEM study. All peaks in the XRD pattern of nanowires scratched off the substrate were also assigned to planes of α - Ge_3N_4 phase, as is seen in Figure 7(a). However, if XRD patterns were taken from NWs which were still attached to the Ge source, then in addition to alpha phase, the presence of a small amount of β - Ge_3N_4 phase was found, together with weak peaks attributed to the Ge source underneath (Figure 7(b)). These results indicated that β - Ge_3N_4 XRD peaks originate from the surface of Ge source and nearby regions. The same situation was observed in [40] for Si_3N_4 NWs. The peaks of α - and β - Si_3N_4 were found in XRD spectrum, while only α - Si_3N_4 phases were detected by TEM investigation of nanowires. Unfortunately, the authors left these results without explanation.

To shed light on this phenomenon, we performed an additional TEM experiment, aimed at the analysis of roots from which the nanowires grew after nucleation (Figures 3(a) and 3(b)). One such root is represented in Figure 7(c). It consists of a close “loop” and two upward directed branches of α - Ge_3N_4 nanowires. The “loop” was initially attached to the GeO_x cluster and its points marked by letters from “d” to “f” were analyzed by high resolution TEM. As can be seen in Figures 7(d)–7(f), the “loop” comprises different phases with clearly defined boundaries. More detailed investigation reveals that α - and β - Ge_3N_4 phases coexist in the “loop.” One example of two-phased nanostructure and its fast Fourier transform is presented in Figures 7(d) and 7(g). The Fourier transform image was used to calculate the d-spacings and two sets of points representing α - and β - Ge_3N_4 phases are shown in Figure 7(g). In contrast to this, the upward directed nanowires in Figure 7(c) have a single crystal structure of α - Ge_3N_4 . It seems that at the initial stage, both α - and β - Ge_3N_4 phases are formed in the nanowire roots. However, the β phase blocks the one-dimensional growth of nanowires and remains in the roots, while the α -phase grows in the form of 1D nanostructure. We suppose that small regions of β - Ge_3N_4 phase may also exist at the surfaces of GeO_x clusters from which the nanowires grow.

4. Conclusions

The hydrazine vapor was used for producing Ge_3N_4 nanowires on the surface of Ge source in the temperature range of 480 – 580°C . The maximum growth temperature of Ge_3N_4 used in our experimental setup was by 300°C lower than the growth temperature of the same type Ge_3N_4 nanostructures obtained in ammonia [13, 14]. This proves

that the hydrazine vapor has a unique role and a high activity in the processes of nitride formation.

At relatively low temperatures not exceeding 520°C, the nanowires were growing through the VLS mechanism with Ge-enriched GeO_x catalyst droplet at the end. At elevated temperatures up to 580°C, the growth was accomplished through the Vapor-Solid mechanism, and Ge₃N₄ nanobelts were produced. The nanowires grown with both methods exhibited the α-Ge₃N₄ structure. The nucleation of Ge₃N₄ was performed on the surface of GeO_x cluster by the formation of both α- and β-Ge₃N₄ phases. However, the one-dimensional growth was observed only for the α-Ge₃N₄ phase.

Acknowledgments

A part of this work was financially supported by the Swiss National Science Foundation through its SCOPES Grant no. IZ73Z0_127943. The authors are thankful to Professor Dr. Greta R. Patzke and Dr. Roman Kontic (University of Zurich, Institute of Inorganic Chemistry, Zurich, Switzerland) for permanent help in experimental work and discussions.

References

- [1] S.-L. Zhang, W. Wang, E.-H. Zhang, and W. Xiao, "Half-metallic ferromagnetism in transition-metal doped germanium nitride: a first-principles study," *Physics Letters A*, vol. 374, no. 31-32, pp. 3234–3237, 2010.
- [2] M. Yang, S. J. Wang, Y. P. Feng, G. W. Peng, and Y. Y. Sun, "Electronic structure of germanium nitride considered for gate dielectrics," *Journal of Applied Physics*, vol. 102, no. 1, Article ID 013507, 6 pages, 2007.
- [3] R. Lieten, S. Degroote, and G. Borghs, United States patent no. 8017509, 2011.
- [4] M. Yang, S. J. Wang, G. W. Peng, R. Q. Wu, and Y. P. Feng, "Ab initio study on intrinsic defect properties of germanium nitride considered for gate dielectric," *Applied Physics Letters*, vol. 91, Article ID 132906, 3 pages, 2007.
- [5] R. R. Lieten, S. Degroote, M. Kuijk, and G. Borghs, "Crystalline Ge₃N₄ on Ge(111)," *Applied Physics Letters*, vol. 91, no. 22, Article ID 222110, 3 pages, 2007.
- [6] G. Okamoto, K. Kutsuki, T. Hosoi, T. Shimura, and H. Watanabe, "Electrical characteristics of Ge-based metal-insulator-semiconductor devices with Ge₃N₄ dielectrics formed by plasma nitridation," *Journal of Nanoscience and Nanotechnology*, vol. 11, no. 4, pp. 2856–2860, 2011.
- [7] Y. Fukuda, Y. Otani, H. Toyota, and T. Ono, "Trap density of GeN_x/Ge interface fabricated by electron-cyclotron-resonance plasma nitridation," *Applied Physics Letters*, vol. 99, no. 2, Article ID 022902, 3 pages, 2011.
- [8] Y. Fukuda, H. Okamoto, T. Iwasaki et al., "Thermal improvement and stability of Si₃N₄/GeN_x/p- and n-Ge structures prepared by electron-cyclotron-resonance plasma nitridation and sputtering at room temperature," *Japanese Journal of Applied Physics*, vol. 51, Article ID 090204, 3 pages, 2012.
- [9] M. Kumar, M. K. Rajpalke, B. Roul, T. N. Bhat, A. T. Kalghatgi, and S. B. Krupanidhi, "Determination of MBE grown wurtzite GaN/Ge₃N₄/Ge heterojunctions band offset by X-ray photoelectron spectroscopy," *Physica Status Solidi (B)*, vol. 249, no. 1, pp. 58–61, 2012.
- [10] K. Maeda, N. Saito, D. Lu, Y. Inoue, and K. Domen, "Photocatalytic properties of RuO₂-loaded β-Ge₃N₄ for overall water splitting," *Journal of Physical Chemistry C*, vol. 111, no. 12, pp. 4749–4755, 2007.
- [11] G. Amatucci and N. Pereira, U.S. patent 429/218.1, 2001.
- [12] M. S. Somayazulu, K. Leinenweber, H. Hubert, P. F. McMillan, and G. H. Wolf, *Proceedings of 17th AIRAPT Conference: Science and Technology of High Pressure*, Universities Press, Hyderabad, India, 2000.
- [13] Y. H. Gao, Y. Bando, and T. Sato, "Nanobelts of the dielectric material Ge₃N₄," *Applied Physics Letters*, vol. 79, no. 27, pp. 4565–4567, 2001.
- [14] T. Xie, Z. Jiang, G. Wu, X. Fang, G. Li, and L. Zhang, "Characterization and growth mechanism of germanium nitride nanowires prepared by an oxide-assisted method," *Journal of Crystal Growth*, vol. 283, no. 3-4, pp. 286–290, 2005.
- [15] D. Jishiashvili, V. Kapaklis, X. Devaux et al., "Germanium nitride nanowires produced by thermal annealing in hydrazine vapor," *Advanced Science Letters*, vol. 2, no. 1, pp. 40–44, 2009.
- [16] D. Dirtu, L. Odochian, A. Pui, and I. Humelnicu, "Thermal decomposition of ammonia. N₂H₄—an intermediate reaction product," *Central European Journal of Chemistry*, vol. 4, no. 4, pp. 666–673, 2006.
- [17] G. R. Patzke, R. Kontic, Z. Shiolashvili, N. Makhatadze, and D. Jishiashvili, "Hydrazine-assisted formation of indium phosphide (InP)-based nanowires and core-shell composites," *Materials*, vol. 6, pp. 85–100, 2013.
- [18] D. Schmeisser, R. D. Schnell, A. Bogen et al., "Surface oxidation states of germanium," *Surface Science*, vol. 172, no. 2, pp. 455–465, 1986.
- [19] S. J. Wang, J. W. Chai, J. S. Pan, and A. C. H. Huan, "Thermal stability and band alignments for Ge₃N₄ dielectrics on Ge," *Applied Physics Letters*, vol. 89, no. 2, Article ID 022105, 3 pages, 2006.
- [20] K. Kutsuki, G. Okamoto, T. Hosoi, T. Shimura, and H. Watanabe, "Characteristics of pure Ge₃N₄ dielectric layers formed by high-density plasma nitridation," *Japanese Journal of Applied Physics*, vol. 47, no. 4, pp. 2415–2419, 2008.
- [21] D. Jishiashvili, Z. Shiolashvili, V. Gobronidze, and I. Nakhutshvili, "A study of solid phase reactions at the Ge–GeO₂ interface," in *Proceedings of the International Symposium and Exhibition on Advanced Packaging Materials*, pp. 112–115, Stone Mountain Park, Ga, USA, 2002.
- [22] G. Xu, Z. Li, J. Baca, and J. Wu, "Probing nucleation mechanism of self-catalyzed inn nanostructures," *Nanoscale Research Letters*, vol. 5, no. 1, pp. 7–13, 2010.
- [23] S. N. Mohammad, "Analysis of the vapor-liquid-solid mechanism for nanowire growth and a model for this mechanism," *Nano Letters*, vol. 8, no. 5, pp. 1532–1538, 2008.
- [24] R. C. Jaeger, *Thermal Oxidation of Silicon. Introduction to Microelectronic Fabrication*, Prentice Hall, Upper Saddle River, NJ, USA, 2nd edition, 2002.
- [25] N. Tabet, J. Al-Sadah, and M. Salim, "Growth of oxide layer on germanium (011) substrate under dry and wet atmospheres," *Surface Review and Letters*, vol. 6, no. 6, pp. 1053–1060, 1999.
- [26] O. J. Gregory, L. A. Pruitt, E. E. Crisman, C. Roberts, and P. J. Stiles, "Native oxides formed on single-crystal germanium by wet chemical reactions," *Journal of the Electrochemical Society*, vol. 135, no. 4, pp. 923–929, 1988.

- [27] A. Mura, I. Hideshima, Z. Liu, T. Hosoi, H. Watanabe, and K. Arima, "Water growth on GeO₂/Ge(100) stack and its effect on the electronic properties of GeO₂," *The Journal of Physical Chemistry C*, vol. 117, no. 1, pp. 165–171, 2013.
- [28] T.-F. Teng, W.-L. Lee, Y.-F. Chang, J.-C. Jiang, J.-H. Wang, and W.-H. Hung, "Adsorption and thermal reactions of H₂O and H₂S on Ge(100)," *Journal of Physical Chemistry C*, vol. 114, no. 2, pp. 1019–1027, 2010.
- [29] R. F. Lever and F. Jona, "Epitaxial growth of germanium using water vapor," *Journal of Applied Physics*, vol. 34, no. 10, pp. 3139–3140, 1963.
- [30] L. S. Palatnik and I. I. Papiro, *Epitaxial Films*, Nauka, Moscow, Russia, 1971.
- [31] S. M. Cohen, Y. L. Yang, E. Rouchouze, T. Jin, and M. P. D'Evelyn, "Adsorption and decomposition of hydrides on Ge(100)," *Journal of Vacuum Science & Technology A*, vol. 10, no. 4, pp. 2166–2166, 1992.
- [32] T. J. Hsu, Ch. Y. Ko, and W. T. Lin, "Water-vapor-enhanced growth of Ge–GeO_x core-shell nanowires and Si_{1-x}Ge_xO_y nanowires," *Nanotechnology*, vol. 18, Article ID 385601, 4 pages, 2007.
- [33] W.-L. Lo, H.-C. Chang, T.-J. Hsu, and W.-T. Lin, "Effects of Cu catalyst and water vapor on the growth of Ge–GeO_x core-shell nanowires via the carbothermal reduction of GeO₂ powders," *Japanese Journal of Applied Physics*, vol. 47, no. 4, pp. 3299–3302, 2008.
- [34] E. Sutter, B. Ozturk, and P. Sutter, "Selective growth of Ge nanowires by low-temperature thermal evaporation," *Nanotechnology*, vol. 19, no. 43, Article ID 435607, 5 pages, 2008.
- [35] C. J. Sahle, M. Zschintzsch, C. Sternemann et al., "Influence of hydrogen on thermally induced phase separation in GeO/SiO₂ multilayers," *Nanotechnology*, vol. 22, no. 12, Article ID 125709, 4 pages, 2011.
- [36] S. N. Ruddlesden and P. Popper, "On the crystal structure of the nitrides of silicon and germanium," *Acta Crystallographica*, vol. 11, pp. 465–468, 1958.
- [37] J. W. Mullin, *Crystallization*, Reed Educational and Professional Publishing Ltd, Woburn, Mass, USA, 4th edition, 2001.
- [38] B. Molina and L. E. Sansores, "Electronic structures of Ge₃N₄—possible structures," *The International Journal of Quantum Chemistry*, vol. 80, pp. 249–257, 2000.
- [39] Y. Ming, *Surface passivation and high-k dielectrics integration of Ge-based FETs: first-principles calculations and in situ characterizations [Ph.D. thesis]*, National University of Singapore, 2009.
- [40] W. Yang, Z. Xie, H. Miao, L. Zhang, H. Ji, and L. An, "Synthesis of single-crystalline silicon nitride nanobelts via catalyst-assisted pyrolysis of a polysilazane," *Journal of the American Ceramic Society*, vol. 88, no. 2, pp. 466–469, 2005.



Hindawi

Submit your manuscripts at
<http://www.hindawi.com>

